RPE | Radiation Physics & Engineering
A Peer-Reviewed Journal
Published by K.N. Toosi University of Technology
http://rpe.kntu.ac.ir
Research Article

Radiation Physics and Engineering 2025; 6(4):47–53

Investigating the impact of radon therapy in water and air on the population density of stem cells

Gita Abedi*, Mohammadreza Rezaie, Marjan Atghaie

Department of Nuclear Engineering, Faculty of Modern Sciences and Technologies, Graduate University of Advanced Technology, Kerman, Iran

HIGHLIGHTS

- Investigation of radon's impact on stem cell population density using MCNPX and the 4^{th} order Runge-Kutta method.
- Simulation of radon dosimetry in a MIRD phantom to study its effects on organs.
- Reduction of 2.65% in air and 12.33% in water in stem cell density observed after 4 days of radon exposure.
- Application of radon therapy as a potential treatment for skin and lung diseases despite its carcinogenic effects.

ABSTRACT

Despite the negative effects of radon on lung and skin cancers, it is possible to use radon in the treatment of skin and lung diseases as radon therapy. In this study, using MCNPX simulated dosimetry results for radon in the organs of a MIRD phantom, an attempt was made to investigate changes in the rate of stem cell population density. The dose rate in the air and water was calculated and incorporated into the differential equation of the stem cells, and then this equation was solved using the 4^{th} order Runge-Kutta method. The results show that radon dose reduces the population density of stem cells over a period of 4 days. At the end of day 4, the stem cell density for a person in the air and water had decreased by 2.65 percent and 12.33 percent, respectively.

KEYWORDS

Radon
Radon Therapy
Dosimetry
MIRD Phantom
MCNPX
Fourth-Order Runge-Kutta
Stem cells

HISTORY

Received: 3 June 2025
Revised: 20 August 2025
Accepted: 3 September 2025
Published: Autumn 2025

1 Introduction

Radon generally causes lung and skin cancers, and is the second leading cause of death worldwide (Nunes et al., 2022). This is true even though a person is constantly exposed to alpha radiation from radon and its daughters (Degu Belete and Alemu Anteneh, 2021). In a situation where the space is assumed to be free of radon, the benefits of radon treatment can be enjoyed for a limited time by exposing the body to water or air (Dobrzyńska et al., 2023). In recent years, significant advances have been made in computational modeling of radiation biology. For example, Rory-Ray Liu and colleagues have presented a robust agent-based model that is able to simulate the response of cells after radiation and enable digital experiments in the context of a "digital twin" for personalized radiotherapy treatments (Liu et al., 2025). Now, returning to our discussion, a common method in radon therapy is to place people in special chambers for treatment (Maccarone et al., 2023). In this case, radon radiation is emitted from granite or radioactive rocks, and the radon concentration increases for radon therapy compared to the closed space used (Domingos et al., 2021). This research attempted to examine the rate of stem cell population density. For this purpose, first a MIRD phantom is considered in the MCNPX code, which is a nuclear atomic code capable of tracking 32 atomic and nuclear particles, in water and air environments (Elshami et al., 2021; Tekin et al., 2022; Lehner et al., 2025). Stem cells, due to their unique ability for self-renewal and differentiation into specialized cell types, play a crucial role in regenerative medicine and the treatment of otherwise incurable diseases (Poliwoda

*Corresponding author: g.abedi@student.kgut.ac.ir

https://doi.org/10.22034/rpe.2025.527986.1276

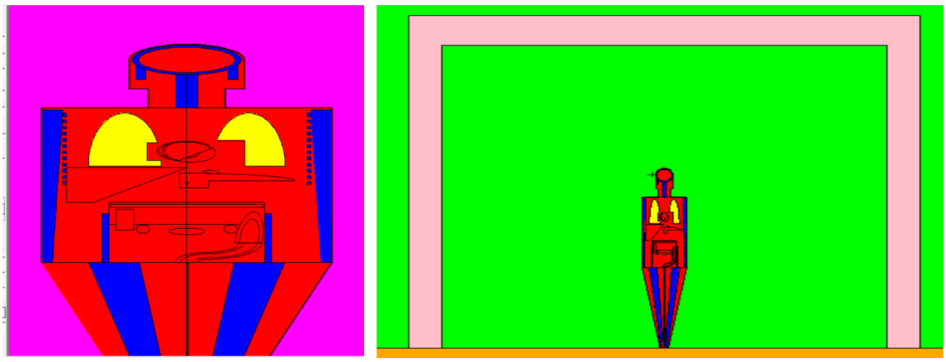

Figure 1: MIRD Phantom.

et al., 2022). They are classified according to their differentiation potential into totipotent, pluripotent, multipotent, oligopotent, and unipotent types, and by their origin into embryonic and adult stem cells (Zakrzewski et al., 2019; Poliwoda et al., 2022). Common sources include bone marrow, umbilical cord blood, adipose tissue, placenta, and neural tissue, each offering broad clinical applications in transplantation, tissue regeneration, and chronic disease treatment (Zakrzewski et al., 2019; Trounson and McDonald, 2015). By calculating the dose in the body's organs, its effects on blood equations, especially the stem cell equation, are interpreted and examined using the 4^{th}-order Runge-Kutta method (DArienzo and Raritià, 2024; Takács et al., 2024). There are many methods for solving differential equations, of which the Runge-Kutta method is considered one of the most efficient (Tan and Chen, 2012).

To solve differential equations using the Runge-Kutta method, validation tests are needed to confirm the method. Therefore, an attempt is made to extract the temporal behavior of WT and Lnk stem cells based on the research of other researchers and calculate the coefficients specific to the stem cell differential equations using the Runge-Kutta method (Suzuki et al., 2012). In scientific research, the distinction between WT (Wild Type) and Lnk-deficient stem cells is pivotal for understanding the mechanisms that control cell behavior. WT stem cells represent the natural state and are regulated by the Lnk protein, which acts as a crucial negative regulator to prevent excessive proliferation of hematopoietic stem cells and maintain bodily homeostasis (Bersenev et al., 2008). Conversely, Lnk-deficient cells, lacking this protein, exhibit hyperactive growth signaling, resulting in significantly increased proliferation and self-renewal (Bersenev et al., 2012). The data obtained in this study were analyzed and reviewed using Origin software. The method of this research will be explained in the following sections.

2 Materials and Methods

This research was conducted in five stages. In the first step, by placing a MIRD phantom in the input file of the MCNPX code in the air, taking into account the equilibrium coefficients of radon and its daughters, the daily dose rate is calculated. Then the temporal behavior of stem cells is extracted from reliable sources. By solving the differential equation of stem cells using the Runge-Kutta method, an attempt is made to modify the existing coefficients so that the results are consistent with the valid extracted data. The effect of the dose of radon and its daughters in the air on the stem cell equation is examined using the 4^{th}-order Runge-Kutta method. Figure 1 shows the Phantom Mird in air.

The dimensions of the space around the MIRD phantom are assumed to be within the range of a 7.69 MeV alpha particle in air. For the Mird phantom in water, the space around the phantom is considered to be about 50 m, which is equal to the alpha range of 7.69 MeV in water. In this case, the body surface area of an adult is 14553 cm^2, which is obtained from Eq. (1) (Burton, 2008):

$$= \text{Body surface area} \tag{1}$$

When the human body, whose surface area is 14,553 cm^3, is placed in water, the alpha decaying radon reaches the body from a maximum depth of 50 μm, which is the alpha range of 7.69 MeV in water. As a result, the active volume of radon decay around the body is equal to this surface area multiplied by 50 μm, i.e. $V_{water} = 14553 \times 50 \times 10^{-4} \approx 72$ cm^3. Also, when a human is in the air, the reason is that the alpha range of 7.69 MeV in the air is due to the decay of radon daughters equal to 6 cm. The active volume around the body will be equal to this surface multiplied by 7.5 cm (Rezaie et al., 2013) i.e. $V_{air} = 14553 \times 7.5 = 109148$ cm^3. In this case, the volume around the phantom will be 109148 cm^3 for air and 72 cm^3 for water according to the MCNPX code data. For air, the concentration of radon is assumed to be 1 Bq.m^{-3} and for water, it is assumed to be 1 kBq.m^{-3}.

The reason for this difference is that the concentration of radon in air is about 1 Bq.m^{-3}, and in water it is about 1 kBq.m^{-3}. For example, the concentration of radon in the fresh air of Khorramabad is about 148 Bq.m^{-3} (Namvaran and Negarestani, 2013) and in the hot spring of Kerman is 42 kBq.m^{-3} (Hassanvand et al., 2018). Also, in the formulation that will be presented later, the radon concentration can be set to any desired value according to the measured article, and this assumption will not affect the results. It is presented solely for the purpose of formulating this assumption. The radon activity in the space around the MIRD phantom is obtained from the equation

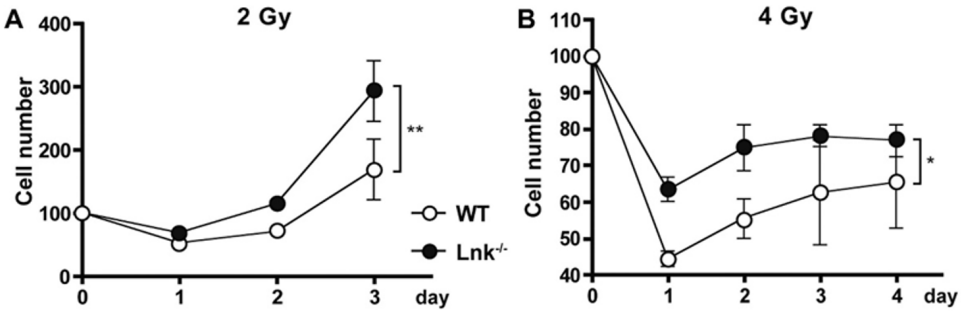

Figure 2: Temporal behavior of WT and Lnk stem cells over time (Suzuki et al., 2012).

$A = CV$. In this study, the total activity of radon in the vicinity of the phantom was calculated using the relation $A = C \times V$, where A is the total activity in becquerels, C (Bq.m^{-3}) is the radon concentration, and V (m^3) is the considered volume. This basic equation is commonly applied in radiation dosimetry to convert measured activity concentrations into total activity values for dose assessment purposes (Knoll, 2010). The dose rate in different organs of MIRD is obtained according to the formula *f6 in MeV.g^{-1}, which is multiplied by 1.6×10^{-10} to convert it to Gy. The factor 1.6×10^{-10} was applied to convert energy deposition values from MeV.g^{-1} to Gy. This constant originates from the relation 1 MeV$= 1.6 \times 10^{-13}$ J and 1 g $=10^{-3}$ kg, and is independent of the medium (air or water) or the activity concentration.

Any differences in the calculated dose are due to variations in radon activity concentration and geometry, rather than the conversion factor (Knoll, 2010). By summing the doses in different organs, the dose of alpha particles in the MIRD phantom will be calculated. The source in question is an alpha source with energies of 5.49, 6, and 7.69 MeV, and the coefficient of each source is considered to be 0.723 and 0.217, respectively, based on the equilibrium coefficients between radon and its daughters. The equilibrium factor (F) is defined as the ratio of the alpha potential energy concentration of radon to the alpha potential energy concentration of radon gas in equilibrium with its product. In simple terms, this factor indicates how "close" radon and its short-lived decay products are to equilibrium in a given environment. These values are 1, 0.723, and 0.217 for radon, Po-218, and Po-214, respectively, meaning that the activities of Po-218 and Po-214 are 72.3% and 21.7%, respectively, of the activities that would exist in complete equilibrium with radon. It should be noted that these percentages are relative to radon, which is itself considered to be a factor of 100%, so the equilibrium factors for radon and its daughters are considered to be 1, 0.723, and 0.217. Most of the time, the number 1 is not mentioned and only the numbers 0.723 and 0.217 are considered.

2.1 Source Definition in MCNPX Simulation

The radiation source was modeled as a uniform volumetric source distributed around the MIRD phantom in both air and water environments. The geometry of the source volume was defined based on the alpha particle range of the radon decay chain. For the air environment, a volume of 109148 cm^3 with a depth of 7.5 cm was used. For the water environment, the source was defined within a volume of 72 cm^3 with a depth of 50 m around the phantom, corresponding to the alpha range in water. Within this source volume, three primary alpha particle energies from the radon decay chain were considered: 5.49 MeV (from Rn-222), 6 MeV (from Po-218), and 7.69 MeV (from Po-214). The probability of each energy was determined based on the equilibrium coefficients (or calibration factors) for radon and its progeny. A total of 1.94 alpha decays were considered for every single radon decay. The probabilities for each energy were calculated to be 0.5154 for the 5.49 MeV alpha, 0.3798 for the 6 MeV alpha, and 0.1140 for the 7.69 MeV alpha. For the dose calculation, the MCNPX input was configured with a source corresponding to one alpha particle emission. The results of this simulation were then scaled to the desired radon concentrations: 1 Bq.cm^{-3} for air and 1 kBq.cm^{-3} for water. The concentration for a single radon decay was defined as 0.5 Bq divided by the phantom's respective volume in air or water, and then converted to the Bq.cm^{-3} unit by converting cm3 to m3. This methodology allowed for a precise calculation of the dose rates in the MIRD phantom corresponding to the specified radon concentrations.

The temporal behavior of stem cells according to reliable sources is shown in Fig. 2. This figure shows the behavior of two types of stem cells, WT and Lnk, over time (Suzuki et al., 2012).

2.2 Stem cell equation

Equation (2) represents the differential equation for stem cells in bone marrow (Khandaker et al., 2023). the coefficients are explained in Table 1 and their units and values are also mentioned.

$$\frac{\mathrm{d}x_1^{ud}}{\mathrm{d}t} = \frac{\alpha\, x_1^{ud}}{1 + \beta(x_1 + \theta_2 x_2 + \theta_3 x_3)} - \gamma x_1^{ud} - \frac{N}{D_1} x_1^{ud} \quad (2)$$

The parameter β is obtained by the relation $\beta = \dfrac{G}{HK}$ where H is the specific rate of natural macrodegradation, G is the macroproduction rate, and K is the inhibition constant. This equation shows that stem cells are produced at a rate of γ and transformed into other types of

Table 1: Coefficients of blood stem cell production parameters (Fedorov, 1976).

Parameter	Value	Unit	Explanation
α	2.4	day^{-1}	Stem cell production rate in bone marrow
γ	1.4	day^{-1}	Stem cell differentiation rate into progenitors
β	0.00018	day^{-1}	Death rate of progenitor cells
D_1	AIR: $2.6E-09$ WATER: 1E-11	Gy	Reference dose for studying of the radiation effect on stem cells due radon in air and water
θ_2	0	Without unit	Coefficient dependent on the effect of radiation on the second stage
θ_3	0	Without unit	Coefficient dependent on the effect of radiation on the third stage

cells at a rate of $\frac{\alpha x_1^{ud}}{1+\beta(x_1+\theta_2 x_2+\theta_3 x_3)}$ and also some of them are destroyed at a rate of $\frac{N}{D_1}$ (Fedorov, 1976).

In this equation, the coefficient γ is equal to 1.4 day^{-1}, N is the dose rate in terms of $Gy.day^{-1}$ and D_1 is a specific value of the dose in terms of Gy (Fedorov, 1976; Pedersen et al., 2023). According to Fig. 2, the α coefficient was calculated to be 7 for the WT type stem cell and 8 for the Lnk type. Also, the coefficient is considered to be 0.00018 according to the data in Fig. 2. Due to the investigation of the stem cell density and the failure to calculate the density of other cells (x_2 and x_3), the values of the inhibition coefficients θ_2 and θ_3 were taken as zero. The coefficient D_1 was taken as 2.6 nGy for air and 10 pGy for water. The dose rate N is obtained according to Monte Carlo calculations.

2.3 4^{th}-order Rang-Kutta equations

The 4^{th}-order Runge-Kutta method is a method for solving differential equations, the series of which is shown in Eq (3)) (DArienzo and Rarità, 2024).

$$\begin{aligned} K_1 &= hf(x_n, y_n) \\ K_2 &= hf(x_n+\frac{h}{2}, y_n+\frac{K_1}{2}) \\ K_3 &= hf(x_n+\frac{h}{2}, y_n+\frac{K_2}{2}) \\ K_4 &= hf(x_n+h, y_n+K_3) \\ y_n+1 &= y_n+\frac{K_1}{6}+\frac{K_2}{3}+\frac{K_3}{3}+\frac{K_4}{6}+O(h^5)) \end{aligned} \quad (3)$$

In these equations, h is the step of change. By the effect of dose rate in the equations of stem cells, changes in their population density rate can be studied.

3 Results

3.1 Dosimetry results of radon in air and water

The results of MCNPX code dosimetry calculations were performed for an alpha emission resulting from the decay of radon and its progeny in air and water. The results for the various organs of the MIRD phantom receiving doses in terms of $MeV.g^{-1}$ are shown in Tables 2 and 3.

By applying the relevant coefficients, the dose rate of radon and progeny for 1 $Bq.m^{-3}$ radon in air and 1 $kBq.m^{-3}$ radon in water can be calculated. The doses per particle from the source, as presented in Tables 2 and 3, are given in units of $MeV.g^{-1}$. To convert these values into the dose rate in ($Gy.day^{-1}$), the following procedure was used:

First, the total activity (A) of the radon source for concentrations of 1 Bqm^{-3} and 1 $kBq.m^{-3}$ using the formula $A = CV$ was calculated, where C ($Bq.m^{-3}$) is the radon concentration and V (m^3) is the volume around the phantom (that is 72 cm^3 for air and 109148 cm^3 for water). The resulting radon activities for air and water were 9430.34 and 6286.93 Bq respectively. The total dose rate in $Gy.day^{-1}$ was then calculated by multiplying the total dose values from Tables 2 and 3 by these activity values, by the factor of 86400 (to convert second to day), and by the conversion factor for $MeV.g^{-1}$ to Gy (1.6×10^{-10}). This resulted in total dose rates of 6.68 $Gy.day^{-1}$ for air and 5.33 $Gy.day^{-1}$ for water. Finally, based on the D_1 value from Table 1, the N/D_1 coefficient for the 1 $Bq.m^{-3}$ concentration in air and the 1 $kBqm^{-3}$ concentration in water was calculated to be 0.514 day^{-1} and 0.106 day^{-1} respectively. These values allow for the investigation of the impact of radon on both WT and Lnk stem cells.

Table 2: Radon Dose ($MeV.g^{-1}$) per particle in air.

Radon in air		
Cell	Volume (g)	Dose ($MeV.g^{-1}$) per particle
Trunk	4.48136E+04	2.69246E-08
Head	5.46000E+03	1.44031E-10
Legs	2.16320E+04	8.80611E-08
Lower colon Descending colon Sigmoid colon	3.09816E+02	3.95638E-09
Scalp and neck	3.30720E+02	1.65557E-04
Trunk skin	1.49760E+03	1.18240E-04
Feet skin	1.25840E+03	1.58762E-04
Total Dose		4.43E-04

Table 3: Radon Dose ($MeV.g^{-1}$) per particle in water.

Radon in water		
Cell	Volume (g)	Dose ($MeV.g^{-1}$) per particle
Legs	2.16320E+04	2.16428E-10
Scalp and neck	3.30720E+02	1.66523E-07
Trunk skin	1.49760E+03	1.86386E-07
Feet skin	1.25840E+03	1.76468E-07
Total Dose		5.30E-07

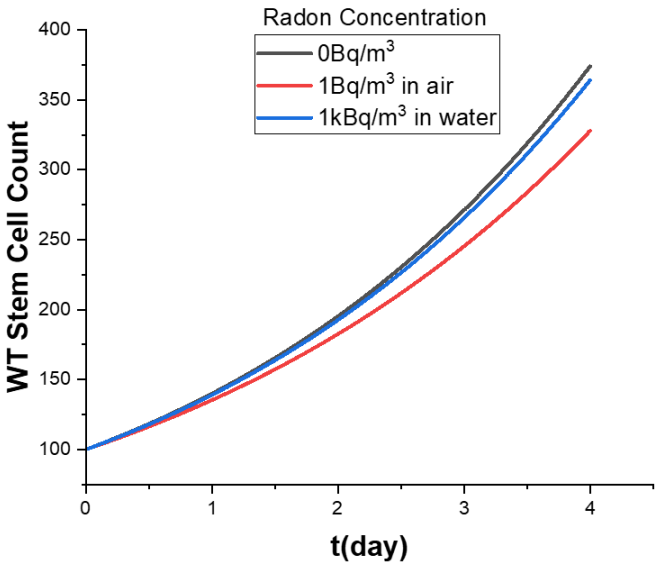

Figure 3: Changes in WT stem cells in air and water.

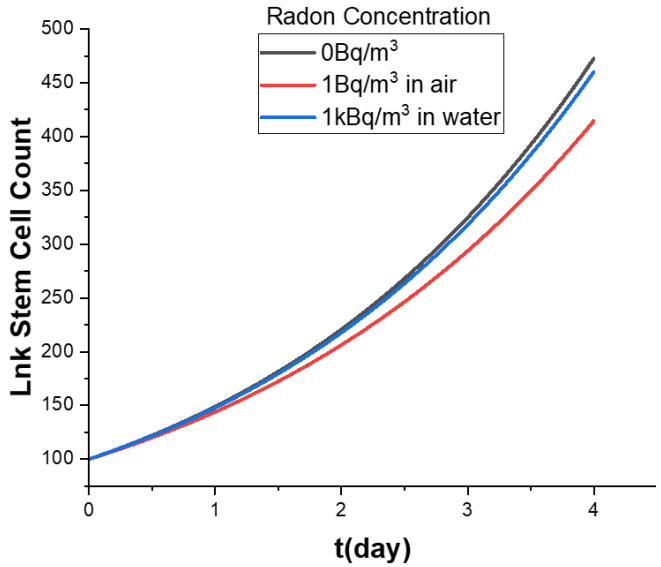

Figure 4: Changes in Lnk-type stem cells in air and water.

3.2 The variation of stem cells population in effect of radon in air and water

According the radon dose rate calculations in the air and water for WT and Lnk stem cells due 1 Bq.m^{-3} radon in air and 1 kBq.m^{-3} radon in water, the rate of change in stem cell population density were calculated using the 4th order Runge-Kutta method, the graphs of which are shown in Figs. 3 and 4.

Examining the graphs in Figs. 3 and 4 shows that the rate of stem cell change in air is greater than in water due to the higher dose of radon and its progeny in the air.

Figures 3 and 4 show the proliferation of WT and Lnk stem cells over four days exposed to different concentrations of radon. The graphs show three distinct scenarios: a control group without radon (0 Bq.m^{-3}) and two experimental groups exposed to radon concentrations of 1 kBq.m^{-3} in water and 1 Bq.m^{-3} in air. A key observation from both figures is that Lnk stem cells (Fig. 4) show a significantly higher proliferation rate and a more pronounced curve curvature compared to WT stem cells (Fig. 3). In contrast, the difference between the radonexposed and control groups appears minimal in both figures. This can be attributed to the low dose effect of radiation. Even at a concentration of 1 kBq.m^{-3}, the dose received by the cells is in a range that the robust DNA repair mechanisms of stem cells can effectively mitigate. The small changes observed are a direct result of a key parameter of the model, the N/D_1 factor, which quantifies the rate of cell loss due to radiation. Our calculations showed that this factor remains a minor factor compared to natural cell proliferation, leading to similar growth curves as seen in the figures. Our findings demonstrate that over a one-day period, the impact of radon on the population density of stem cells is minimal. This suggests that low-dose, short-term exposure, such as that used in radon therapy, may not significantly disrupt normal stem cell proliferation, a critical factor for tissue health and repair. Historically, radon therapy has been considered a potential treatment modality for various skin and respiratory diseases, despite its well-established association with lung and skin cancer risks. The minimal change observed in our in-vitro model over a short duration provides a preliminary basis for understanding why low-dose radon exposure might be tolerated in clinical settings, supporting its potential as a therapeutic approach while highlighting the importance of carefully controlled exposure duration and concentration to avoid long-term risks.

4 Discussion

Radon therapy has been historically considered as a potential modality for the treatment of various skin and respiratory diseases, despite its well-established association with lung and skin cancer risks. In this study, computational dosimetry data obtained from MCNPX simulations in an MIRD phantom were used to investigate the biological effects of radon exposure on stem cell population density. The absorbed dose by different organs was calculated under two exposure scenarios -water and air- and then incorporated into a differential equation modeling stem cell dynamics, solved via the fourth-order Runge-Kutta method. The results indicate that exposure to radon and its progeny leads to a decrease in the population density of both WT and Lnk types of hematopoietic stem cells over a four-day period. Specifically, at the end of the exposure period, the density of stem cells decreased by approximately 2.65% in the air environment and 12.33% in the water environment

Radon therapy, when applied in controlled low doses and within specific timeframes, has been demonstrated to induce beneficial physiological effects, particularly by modulating inflammatory responses and enhancing regenerative processes. The moderate reductions observed in stem cell populations -2.65% and 12.33%- during the course of radon therapy should be interpreted as part of the body's adaptive hormetic response rather than as indi-

cators of permanent cellular damage (Calabrese and Mattson, 2017; Feinendegen, 2005; Mitsunobu et al., 2003). These transient decreases likely reflect a temporary redistribution or activation of stem cells that contribute to tissue repair and homeostasis. Supporting this, previous studies have shown that low-dose radon exposure can stimulate the production of cytokines and growth factors, which promote stem cell activation and proliferation (Kataoka et al., 2021).

Furthermore, therapeutic radon exposure contrasts with the detrimental effects of chronic, uncontrolled radon exposure. In clinical settings, radon therapy has been associated with improved markers of inflammation and enhanced tissue regeneration without evidence of long-term harm (Falkenbach et al., 2005). This evidence supports the notion that radon therapy, by triggering controlled biological stress, activates endogenous repair mechanisms, thereby offering potential therapeutic benefits.

This disparity in effect can be attributed to the higher concentration and penetration of radon in air compared to water, resulting in greater radiation doses delivered to the body. These findings are consistent with previous studies suggesting that low-dose ionizing radiation may have suppressive effects on hematopoietic stem cells (Khandaker et al., 2023). However, it is important to note that the observed changes were relatively small, particularly in the water exposure scenario, suggesting that radon therapy may not significantly alter systemic stem cell populations under the conditions studied. One of the strengths of this study lies in the use of the MIRD phantom and MCNPX code, which allowed for precise organ-specific dose calculations and enhanced the reliability of the simulation. Moreover, the application of the Runge-Kutta method provided a robust numerical approach for modeling the temporal behavior of stem cell populations under radiation stress. Future studies should consider incorporating in vivo models or clinical data to validate these simulated outcomes. Additionally, exploring the potential protective role of antioxidants or other radioprotective agents during radon therapy could provide further insights into minimizing adverse biological effects while preserving therapeutic benefits.

5 Conclusions

This study investigated the impact of short-term radon therapy in water and air environments on the population density of hematopoietic stem cells using dosimetric data derived from MCNPX simulations in an MIRD phantom. The results demonstrated a modest reduction in stem cell density following exposure, with a more pronounced effect observed in the air environment compared to the water environment. While radon therapy remains a topic of interest in alternative medicine, the findings suggest that its influence on stem cell population density is minimal within the parameters examined. These results contribute to the growing understanding of radons biological effects and underscore the importance of careful dosimetry in evaluating the safety and efficacy of radon-based therapies. Further research integrating clinical observations and long-term follow-up is recommended to comprehensively assess the implications of radon exposure on stem cell dynamics and overall health outcomes.

Conflict of Interest

The authors declare no potential conflict of interest regarding the publication of this work.

Funding

The authors declare that no funds, grants, or other financial support were received during the preparation of this manuscript.

References

Bersenev, A., Rozenova, K., Balcerek, J., et al. (2012). Lnk deficiency partially mitigates hematopoietic stem cell aging. *Aging Cell*, 11(6):949–959.

Bersenev, A., Wu, C., Balcerek, J., et al. (2008). Lnk controls mouse hematopoietic stem cell self-renewal and quiescence through direct interactions with JAK2. *The Journal of Clinical Investigation*, 118(8):2832–2844.

Burton, R. F. (2008). Estimating body surface area from mass and height: theory and the formula of Du Bois and Du Bois. *Annals of Human Biology*, 35(2):170–184.

Calabrese, E. J. and Mattson, M. P. (2017). How does hormesis impact biology, toxicology, and medicine? *NPJ Aging and Mechanisms of Disease*, 3(1):13.

DArienzo, M. P. and Raritá, L. (2024). Dynamics of Blood Flows in the Cardiocirculatory System. *Computation*, 12(10):194.

Degu Belete, G. and Alemu Anteneh, Y. (2021). General overview of radon studies in health hazard perspectives. *Journal of Oncology*, 2021(1):6659795.

Dobrzyńska, M. M., Gajowik, A., and Wieprzowski, K. (2023). Radon–occurrence and impact on the health. *Roczniki Państwowego Zakładu Higieny*, 74(1):5–14.

Domingos, F. P., Sêco, S. L., and Pereira, A. J. (2021). Thoron and radon exhalation and emanation from granitic rocks outcropping in the Central Iberian Zone (Portugal). *Environmental Earth Sciences*, 80(22):753.

Elshami, W., Tekin, H. O., Issa, S. A., et al. (2021). Impact of eye and breast shielding on organ doses during cervical spine radiography: design and validation of MIRD computational phantom. *Frontiers in Public Health*, 9:751577.

Falkenbach, A., Kovacs, J., Franke, A., et al. (2005). Radon therapy for the treatment of rheumatic diseasesreview and meta-analysis of controlled clinical trials. *Rheumatology International*, 25(3):205–210.

Fedorov, N. (1976). Normal haemopoiesis and its regulation. *Moscow: Meditsina*, pages 98–510.

Feinendegen, L. (2005). Evidence for beneficial low level radiation effects and radiation hormesis. *The British Journal of Radiology*, 78(925):3–7.

Hassanvand, H., Sadegh Hassanvand, M., Birjandi, M., et al. (2018). Indoor radon measurement in dwellings of Khorramabad city, Iran. *Iranian Journal of Medical Physics*, 15:19–27.

Kataoka, T., Naoe, S., Murakami, K., et al. (2021). Mechanisms of action of radon therapy on cytokine levels in normal mice and rheumatoid arthritis mouse model. *Journal of Clinical Biochemistry and Nutrition*, 70(2):154.

Khandaker, M. U., Hassanpour, M., Khezripour, S., et al. (2023). Investigation of the effect of I-131 on blood parameters for thyroid cancer treatment. *Radiation Physics and Chemistry*, 208:110897.

Knoll, G. F. (2010). *Radiation detection and measurement*. John Wiley & Sons.

Lehner, F., Lombardo, P., Castillo, S., et al. (2025). RadField3D: a data generator and data format for deep learning in radiation-protection dosimetry for medical applications. *Journal of Radiological Protection*, 45(2):021508.

Liu, R., Swat, M. H., Glazier, J. A., et al. (2025). Developing an Agent-Based Mathematical Model for Simulating Post-Irradiation Cellular Response: A Crucial Component of a Digital Twin Framework for Personalized Radiation Treatment. *arXiv preprint arXiv:2501.11875*.

Maccarone, M. C., Scanu, A., Coraci, D., et al. (2023). The potential role of spa therapy in managing frailty in rheumatic patients: A scoping review. In *Healthcare*, volume 11, page 1899. MDPI.

Mitsunobu, F., Yamaoka, K., Hanamoto, K., et al. (2003). Elevation of antioxidant enzymes in the clinical effects of radon and thermal therapy for bronchial asthma. *Journal of Radiation Research*, 44(2):95–99.

Namvaran, M. and Negarestani, A. (2013). Measuring the radon concentration and investigating the mechanism of decline prior an earthquake (Jooshan, SE of Iran). *Journal of Radioanalytical and Nuclear Chemistry*, 298(1):1–8.

Nunes, L. J., Curado, A., Graça, L. C. d., et al. (2022). Impacts of indoor radon on health: a comprehensive review on causes, assessment and remediation strategies. *International Journal of Environmental Research and Public Health*, 19(7):3929.

Pedersen, R. K., Andersen, M., Stiehl, T., et al. (2023). Understanding hematopoietic stem cell dynamicsinsights from mathematical modelling. *Current Stem Cell Reports*, 9(1):9–16.

Poliwoda, S., Noor, N., Downs, E., et al. (2022). Stem cells: a comprehensive review of origins and emerging clinical roles in medical practice. *Orthopedic Reviews*, 14(3):37498.

Rezaie, M. R., Sohrabi, M., Negarestani, A., et al. (2013). Energy of radon and progeny alphas in dependence of distance traveled in some media. *Radiation measurements*, 50:145–148.

Suzuki, N., Yamazaki, S., Ema, H., et al. (2012). Homeostasis of hematopoietic stem cells regulated by the myeloproliferative disease associated-gene product Lnk/Sh2b3 via Bcl-xL. *Experimental Hematology*, 40(2):166–174.

Takács, B. M., Sebestyén, G. S., and Faragó, I. (2024). High-order reliable numerical methods for epidemic models with non-constant recruitment rate. *Applied Numerical Mathematics*, 206:75–93.

Tan, D. and Chen, Z. (2012). On a general formula of fourth order Runge-Kutta method. *Journal of Mathematical Science & Mathematics Education*, 7(2):1–10.

Tekin, H. O., ALMisned, G., Issa, S. A., et al. (2022). A rapid and direct method for half value layer calculations for nuclear safety studies using MCNPX Monte Carlo code. *Nuclear Engineering and Technology*, 54(9):3317–3323.

Trounson, A. and McDonald, C. (2015). Stem cell therapies in clinical trials: progress and challenges. *Cell Stem Cell*, 17(1):11–22.

Zakrzewski, W., Dobrzyński, M., Szymonowicz, M., et al. (2019). Stem cells: past, present, and future. *Stem Cell Research & Therapy*, 10(1):68.

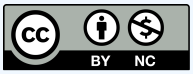

To cite this article:

Abedi, G. , Rezaie, M. and atghaei, M. (2025). Investigating the impact of radon therapy in water and air on the population density of stem cells. *Radiation Physics and Engineering*, 6(4): 47-53. doi: 10.22034/rpe.2025.527986.1276

DOI: 10.22034/rpe.2025.527986.1276

To link to this article: https://doi.org/10.22034/rpe.2025.527986.1276